

- 137 (1980).
13. H. C. Bold and M. J. Wynne, *Introduction to the Algae* (Prentice-Hall, Englewood Cliffs, NJ, ed. 2, 1986); F. E. Fritsch, *The Structure and Reproduction of the Algae* (Cambridge Univ. Press, Cambridge, 1965).
 14. K. M. Cole, C. M. Park, P. E. Reid, R. G. Sheath, *J. Phycol.* **21**, 585 (1985).
 15. K. Cole and E. Conway, *Phycologia* **14**, 239 (1975).
 16. C. D. Walcott, *Smithsonian Misc. Coll.* **67**, 217 (1919); W. L. Fry, *Rev. Palaeobot. Palynol.* **39**, 313 (1983).
 17. T. C. Martin and J. T. Wyatt, *J. Phycol.* **10**, 57 (1974).
 18. S. Golubic, personal communication.
 19. N. J. Butterfield and A. H. Knoll, *Geol. Soc. Am. Abstr. Prog.* **21**, A146 (1989).
 20. N. J. Butterfield, A. H. Knoll, K. Swett, *Nature* **334**, 424 (1988).
 21. T. N. German, *Paleontol. J.* **1981**, no. 2, 100 (1981).
 22. H. J. Hofmann, in *Paleoalgology: Contemporary Research and Applications*, D. F. Toomey and M. H. Nitecki, Eds. (Springer-Verlag, Berlin, 1985), pp. 20–33.
 23. M. R. Walter, J. H. Oehler, D. Z. Oehler, *J. Paleontol.* **50**, 872 (1976); Du Rulin, Tian Lifu, Li Hanbang, *Acta Geol. Sinica* **1986**, no. 2, 115 (1986).
 24. K. Grey and I. R. Williams, *Precamb. Res.* **46**, 307 (1990).
 25. S. W. F. Grant and A. H. Knoll, *Geol. Soc. Am. Abstr. Prog.* **19**, 681 (1987).
 26. Zhang Y., *Lethaia* **22**, 113 (1989).
 27. G. Vidal, *ibid.*, p. 375.
 28. M. B. Gnilovskaya, Ed., *Vendotaenids of the East European Platform* (Nauka, Leningrad, 1988).
 29. S. Campbell, *J. Phycol.* **19**, 25 (1980).
 30. D. Bhattacharya, H. J. Elwood, L. J. Goff, M. L. Sogin, *ibid.* **26**, 181 (1987).
 31. R. Perasso, A. Baroin, L. H. Qu, J. P. Bachelier, A. Adoutte, *Nature* **339**, 142 (1990).
 32. H. Tappan, *Geol. Soc. Am. Bull.* **87**, 633 (1976).
 33. We thank the National Geographic Society, the National Science Foundation, and the Department of Energy for supporting field and laboratory work, and the Canadian Polar Continental Shelf Project for logistic support in the field. S. Golubic first pointed out the bangiophyte habit of the fossil material and D. Bhattacharya provided useful phylogenetic information; the comments of an anonymous reviewer concerning modern *Bangia* biology were particularly instructive. N.J.B. is supported by a Natural Sciences and Engineering Research Council of Canada post-graduate scholarship.

16 April 1990; accepted 25 July 1990

Not So Hot “Hot Spots” in the Oceanic Mantle

ENRICO BONATTI

Excess volcanism and crustal swelling associated with hot spots are generally attributed to thermal plumes upwelling from the mantle. This concept has been tested in the portion of the Mid-Atlantic Ridge between 34° and 45° (Azores hot spot). Peridotite and basalt data indicate that the upper mantle in the hot spot has undergone a high degree of melting relative to the mantle elsewhere in the North Atlantic. However, application of various geothermometers suggests that the temperature of equilibration of peridotites in the mantle was lower, or at least not higher, in the hot spot than elsewhere. The presence of H₂O-rich metasomatized mantle domains, inferred from peridotite and basalt data, would lower the melting temperature of the hot spot mantle and thereby reconcile its high degree of melting with the lack of a mantle temperature anomaly. Thus, some so-called hot spots might be melting anomalies unrelated to abnormally high mantle temperature or thermal plumes.

THE CONCEPT OF HOT SPOTS HAS played an important role in the theory of plate tectonics (1–3). Oceanic hot spots are areas of thicker than normal crust and excess volcanism and are commonly marked by islands. They are generally attributed to anomalously high temperatures of upwelling mantle plumes, which result in overabundant production of melt and in crustal swelling (1–4). In this report I discuss data from one such inferred hot spot, the Azores hot spot complex (AHS), located between 34° and 45°N in the Mid-Atlantic Ridge (MAR). These data imply that this so-called hot spot may not be caused by anomalously high upper-mantle temperatures, but rather by a mantle with a composition different from that underlying normal

segments of the Mid-Atlantic Ridge.

The geochemical nature of the oceanic upper mantle has been inferred from studies of the melts extracted from it (oceanic basalts) or of the solid residue left behind in the mantle after melt extraction (oceanic peridotites). The reconstructed primary mineralogy of oceanic peridotites [olivine + orthopyroxene (opx) ± clinopyroxene (cpx) + spinel] suggests that they equilibrated in the spinel peridotite facies [pressure >8 to 9 kbar at 1000° to 1300°C (5)]. I compare the chemistry of these mantle-equilibrated relic phases in samples of peridotite bodies emplaced in young (<35 million years old) North Atlantic crust (Fig. 1) and representing the uppermost sub-Atlantic mantle [see (6–8) for methods and raw data].

Regional, long-wavelength (~1000 km) variations of peridotite modal and mineral composition (Fig. 2), detected along the

MAR (6, 9), must reflect fundamental regional differences in upper mantle composition, thermal structure, or both (10). The chemistry of the primary minerals, namely their content of Mg, Cr, and other refractory elements versus that of Al, Fe, and other incompatible elements (10–12), suggest that greater amounts of melt [up to >20% melting relative to a pyrolite-like source (6)] have been extracted from the mantle rocks in the AHS region than elsewhere in the MAR, where the degree of melting can be as low as 8% (6). These regional variations along the MAR are associated with variations of geophysical parameters (Fig. 2) such as zero-age sea-floor depth (13) and geoid residual anomaly (14), and basalt properties such as Na₂O content (15) and La/Sm ratio (16). Basalt Na₂O content has been related to the degree of partial melting undergone by the source material in the mantle (15). It is inversely correlated with the 100Cr/(Cr + Al) ratio of spinels in peridotite. Along with other mineral chemistry relations (6), it provides independent support for high degree of melting of the AHS mantle.

This high degree of melting could reflect higher upper-mantle temperatures in the AHS than elsewhere along the MAR, consistent with the notion that the anomalous region is a hot spot (15, 16). If temperature differences in the upper mantle were the sole cause of the different degrees of melting, estimated differences in mantle temperature between mid-ocean ridge segments with highest and lowest extent of melting should be ~250° to ~300°C at equivalent depths in the melting region (15). If we consider only the North Atlantic part of the ridge, these differences are reduced somewhat. The temperature differences would be smaller at shallower depth in the mantle where final subsolidus equilibration of the peridotite occurs, but should still exceed 100°C.

In order to test the assumption that mantle temperature is the cause of differences in the degree of melting along the MAR, I have calculated peridotite equilibration temperatures using the Wells' (17) and Lindsley's (18, 19) geothermometers. Both are based on the temperature dependence of reactions between coexisting opx and cpx (20, 21). Among the various proposed peridotite geothermometers, these appear to be the most reliable, particularly for peridotites equilibrated in the spinel lherzolite stability field (22). However, because of the limitations of these and other peridotite geothermometers, I regard the estimated temperatures (Fig. 2) as expressing relative trends rather than absolute values (23). The calculated temperatures are generally consistent within each geotectonic area (24–26).

Lamont-Doherty Geological Observatory of Columbia University, Palisades, New York 10964.

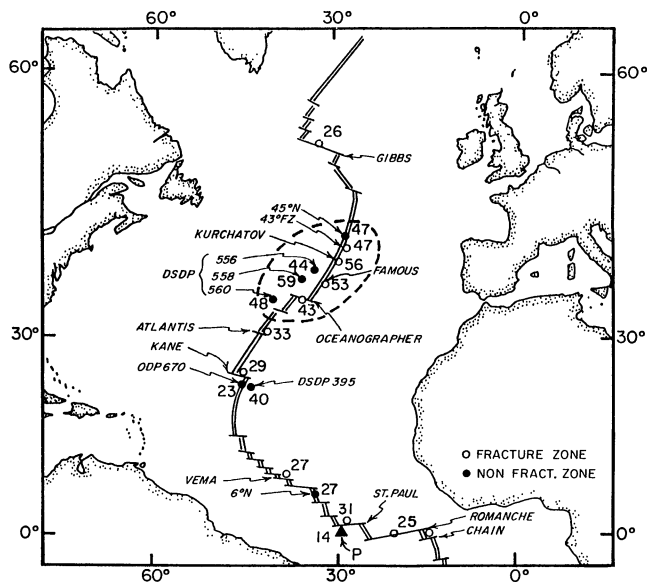


Fig. 1. Areas where peridotite samples were recovered. The spinel $100\text{Cr}/(\text{Cr} + \text{Al})$ ratio of the peridotites is indicated. Numbers represent averages of different samples within the same site, and in the case of fracture zones, of different sites in a fracture zone, as discussed in (6). Peridotites with significant content of plagioclase have not been included. Data are mostly from (6), but also (60) and (61). Data from St. Peter-Paul Island peridotites (black triangle) are from (56). Area enclosed by dashed line indicates schematically the Azores hot spot region.

(MORB) from the AHS region contain two to three times as much H_2O as normal MORB; are enriched in volatiles such as Cl, Br, and F; and tend to have lower SiO_2 content, which is consistent with melting from an H_2O -enriched source (36). This evidence has led Schilling *et al.* (36) to suggest that the AHS behaves also as a “wet spot” and is the locus of metasomatism.

The high La/Sm ratio and general enrichment in light rare-earth elements (LREE) of the AHS basalts (Fig. 2) cannot be explained by increased degrees of melting but requires the addition of an incompatible element-enriched component in the source (16, 37). The abundance of incompatible large-ion lithophile elements (LILE) K, Rb, Cs, Sr, and REE have been estimated in the mantle parental material of normal MAR basalts and in that of AHS basalts for a range of mantle primary modal compositions and of degrees of partial melting (37). This calculation shows that the AHS mantle is strongly enriched in LILE relative to normal MAR mantle (Fig. 3) and that the enrichment is greatest for elements with largest ionic radii (37). These results can be interpreted by considering data obtained from the Zabargad peridotite complex in the Red Sea, a mantle body from a pre-oceanic rift and consisting of undepleted spinel lherzolite veined by metasomatic LILE-enriched

The geothermometry estimates for the peridotites from the AHS, although limited in number by the absence of primary cpx in many of the highly refractory samples, include samples from three areas: Oceanographer fracture zone, 43°N fracture zone, and DSDP Site 556. Average estimated temperatures of equilibration of peridotites from the AHS appear to be lower, or at least not higher, than those of peridotites from elsewhere along the MAR (Fig. 2). The calculated temperatures may actually reflect cooling rates of the upwelling mantle bodies (27).

Experimental work has shown that Al_2O_3 isopleths in opx and the partitioning of Al between opx and spinel in spinel peridotite are controlled primarily by bulk composition and temperature; the partitioning is relatively independent of pressure (22, 28, 29). Thus, peridotites that equilibrated at high temperature should have high Al_2O_3 opx/spinel ratios. However, relatively low values were observed in samples from the AHS region (Fig. 2). These data complement the geothermometry calculations and suggest again that the AHS rocks did not equilibrate at higher temperature than other MAR peridotites.

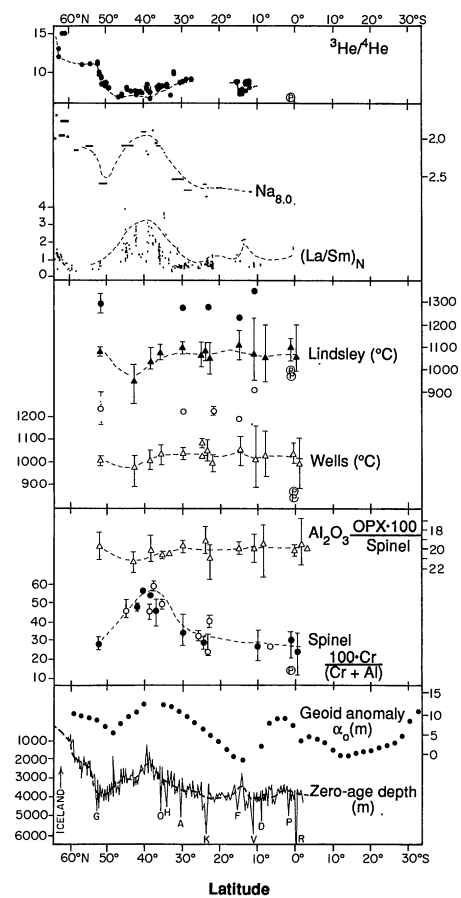
Although the estimated temperatures probably do not represent mantle temperatures during melting but subsolidus re-equilibration temperatures, we would expect them to be higher in a hot spot than in a non-hot spot region. An upper-mantle column above a stable hot spot should be hotter than a column away from a hot spot at equivalent depths. Mantle upwelling and thus cooling rate should be faster in a hot spot than elsewhere and should result in a higher equilibration temperature. These results imply that the high degree of melting of the AHS mantle may not be caused by a

higher mantle temperature than elsewhere along the MAR (27).

The absence of a temperature anomaly could be reconciled with a high degree of melting if the mantle of the AHS was enriched in H_2O and CO_2 . The presence of H_2O and CO_2 (either as free phases or in minerals such as amphiboles, phlogopite, and carbonates) lowers the solidus temperature of peridotite (30–35). This effect is not trivial: even traces of CO_2 or H_2O , or both, can lower the melting temperatures by hundreds of degrees (32). Partial melting would thus be enhanced even in a normal mid-ocean ridge thermal regime.

The notion that the upper mantle in the AHS is enriched in H_2O and other volatiles is supported independently by basalt and peridotite data. Mid-ocean ridge basalts

Fig. 2. Geochemical and geophysical data plotted versus latitude along the northern MAR, from Iceland to the equator. Shown (from the bottom) are: (i) Zero-age crustal depth below sea level, from (13). Major fracture zones are indicated by letters: R, Romanche; P, St. Paul; D, Doldrums; V, Vema; F, $15^\circ 20'$; K, Kane; A, Atlantis; H, Hayes; O, Oceanographer; G, Gibbs. (ii) Residual geoid height anomaly, from (14). (iii) Spinel $100\text{Cr}/(\text{Cr} + \text{Al})$ ratios and the ratio of Al_2O_3 in orthopyroxene to that in spinel of peridotites. Symbols represent average values for each area; bars range of values for each area. Source of data is in Fig. 1. Circled P indicates peridotites from St. Peter-Paul Island (56). (iv) Temperatures of equilibration of peridotites estimated according to Wells (17) and Lindsley (18, 19). Triangles indicate average values and bars the range; circles indicate anomalous high temperatures related to low-Ca, high-Fe cpx. (v) Basalt La/Sm ratio, normalized to chondritic values, from (16); and Na content, normalized to 8% MgO, from (15). The scale for basalt Na content is reversed. (vi) $^3\text{He}/^4\text{He}$ ratio (relative to atmospheric ratio) in MAR basalts and in St. Peter-Paul Island peridotite, from (44) and (58). Shaded band indicates $^3\text{He}/^4\text{He}$ ratio of normal MORB.



amphibole peridotite (38). The LILE distribution of the Zabargad spinel lherzolite plots close to the estimated sub-Atlantic normal parental mantle (Fig. 3A). This result agrees with mineral chemistry and Nd-Sr isotopic data suggesting that the Zabargad spinel lherzolites could be a potential source of MORB (38, 39). The LILE pattern for the Zabargad metasomatic amphibole peridotite plots instead close to the estimated parental mantle for the AHS area (Fig. 3B). That the equivalent of normal oceanic mantle and of hot spot mantle can be found side-by-side as meter-scale heterogeneities in the Zabargad peridotite body supports the notion that a variably veined mantle (40) can also occur beneath the Atlantic, such that the so-called hot spot mantle contains a high proportion of metasomatic component, and the normal ridge mantle a low proportion.

Thus, a variety of data supports the hypothesis that the upper mantle in the AHS area is enriched in H₂O. Wet mantle that upwells adiabatically would cross the wet solidus at a higher pressure than a similar but dry mantle body (Fig. 4). Partial melting during further ascent would lead to cooling because of expenditure of latent heat of fusion (41-43). Because a dry peridotite starts melting at lower pressure, its pressure-temperature (P-T) trajectory during upwelling is displaced toward higher temperature relative to that of the wet peridotite, and should reach final equilibration at a higher temperature. The relatively low equilibration temperatures estimated for the AHS area could thus reflect a subsolidus trajectory at lower temperature because of the H₂O- and CO₂-enrichment relative to the normal MAR mantle.

When and where was this metasomatized mantle created? Basalt ³He/⁴He ratios are lower in the AHS region than in normal MORB (44). This contrasts with most other hot spots such as Hawaii and Iceland, which show ³He/⁴He ratios higher than those in MORB (44-46). The low ³He/⁴He ratio of the AHS area implies that the mantle has either lost ³He (relative to normal MORB mantle) by degassing, or has had an addition of U and Th (44). One possibility is the incorporation in the mantle of old, subducted, partially degassed oceanic crust (44, 47). However, He degassing could result from a metasomatic event (44, 48), which is consistent with the observed enrichment of LILE in the AHS mantle (Fig. 3).

Preferred sites of degassing of the Earth and of mantle metasomatism are continental rifts (48-51) such as the East African-Red Sea rifts where thinning and breaking of the continental lithosphere allows release of mantle volatiles that elsewhere are trapped

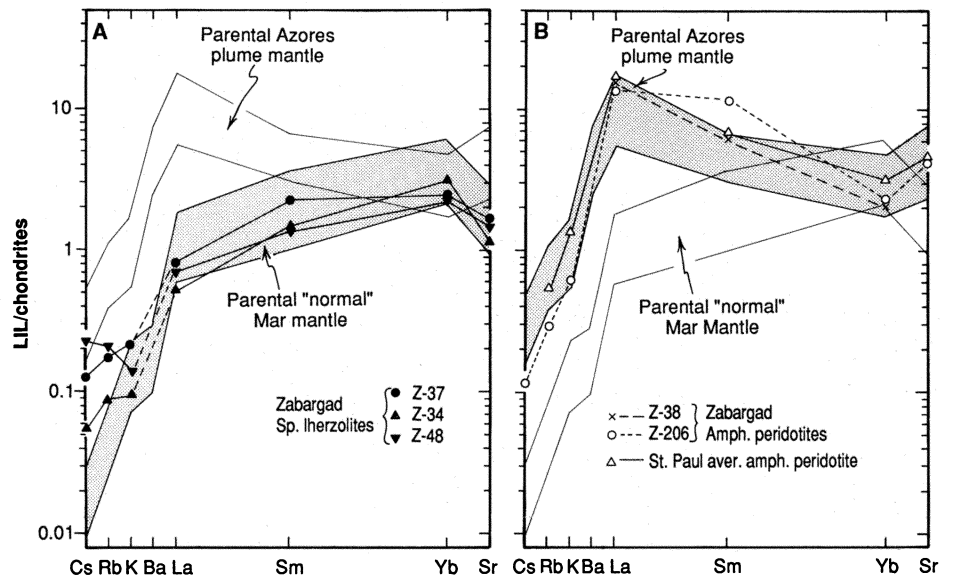


Fig. 3. Estimated chondrite-normalized LIL element content in parental mantle for normal MAR basalts and for AHS basalt, from (37), compared with LIL content of Zabargad spinel lherzolites (A) and of Zabargad metasomatized amphibole (amph.) peridotites (B), from (38, 39). The LIL element distribution of average St. Peter-Paul Island amphibole peridotite, from (56), is also shown.

beneath a thick lithospheric lid. The metasomatized mantle domains inferred for the AHS area might be remnants of proto-Atlantic rift mantle that were left behind during the opening of the North Atlantic. The possibility of having relicts of subcontinental mantle beneath the axial region of the Atlantic has been suggested before (52) and has been proposed recently in order to account for Sr-Nd-Pb isotope systematics of some hot spot oceanic islands (53) and of basalts from the Oceanographer fracture zone (54), well within the AHS area. Basalts from some Atlantic hot spot islands show Sr-Nd-Pb isotope systematics similar to those of East African rift volcanic rocks, for which a metasomatized, H₂O and CO₂-enriched mantle source has been advocated (51).

Direct samples of the inferred metasomatized H₂O-rich mantle domains of the AHS were not obtained, probably because the peridotites from the AHS are highly refractory and the metasomatic components, including mantle-equilibrated amphibole and phlogopite, were extracted during partial melting. However, an example of strongly metasomatized mantle similar to the inferred source of the AHS anomaly has been preserved in the Atlantic islets of St. Peter-Paul (SPP), located near the equator.

The mantle exposed at SPP is a mylonitic spinel peridotite containing variable amounts of amphibole and is associated with hornblende (55, 56). In terms of mineral, trace element, and isotopic chemistry, their undepleted composition, and low estimated temperatures of equilibration (Fig. 2), the SPP peridotites are different from MAR peridotites but similar to those

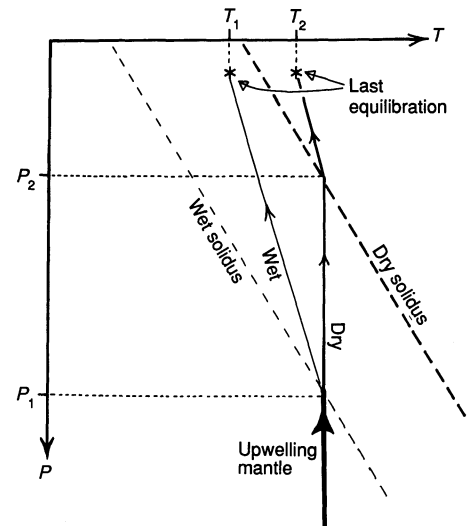


Fig. 4. Qualitative and schematic diagram illustrating partial melting and P-T paths of upwelling "dry" and "wet" peridotitic upper mantle bodies.

at Zabargad (57). Thus, the SPP mantle body may have been spared going through fast upwelling in a hot thermal regime, which would have resulted in higher temperatures of equilibration and in significant partial melting, as is generally seen in MAR peridotites. The LILE distribution of the SPP peridotites (56), just as that of the Zabargad metasomatized amphibole peridotites (38), falls within the range of the estimated mantle source of the AHS basalts (Fig. 3). Moreover, the ³He/⁴He ratio of SPP rocks is lower than that of normal MORB (58) and similar to that of rocks from the AHS area (Fig. 2). In terms of Sr-Nd-Pb isotope systematics, the mantle rocks

at SPP are compatible with the inferred source of ocean island (hot spot) basalt (56) and of East African rift basalt (51). Thus, on the one hand SPP fits the requisites of the mantle source for the AHS basalts. On the other hand, its similarity with the inferred mantle at Zabargad and in the East African rift suggests that SPP might be a fragment of pre-oceanic rift mantle left behind from the opening of the proto-Atlantic rift (57). The probable age of the metasomatic event that affected SPP [155 million years ago (56)] lies within the age of the continental rifting that preceded the opening of the equatorial Atlantic.

The AHS region has positive zero age crustal depth and residual geoid anomalies (Fig. 2). If we assume that there are no temperature differences between the AHS mantle and normal MAR mantle, the AHS axial topographic high must be due to the increased thickness of the crust and of the residual mantle column, in that refractory harzburgite is less dense than fertile lherzolite (59). An additional factor is introduced in these estimates, however, if metasomatized peridotite is abundant in the AHS mantle, because low-density phases would then be abundant. If the metasomatized mantle domains of the AHS region are similar to Zabargad amphibole peridotite with about 20% modal amphibole (38), and with, in addition, phlogopite and carbonates, their density could be lowered close to $\sim 3.2 \text{ g/cm}^3$ relative to that of unmetasomatized (3.3 g/cm^3) spinel lherzolite. The thickness of the metasomatized mantle column would determine the extent of the positive topographic anomaly. The geoid high could then be largely due to topography.

In summary, I suggest that the presence of metasomatized, H_2O - and CO_2 -rich domains in the 34° to 45°N mantle, rather than anomalously high mantle temperatures, can account for the main features of the AHS area, such as (i) the high melting anomaly; (ii) the enriched nature of the basalt; and (iii) the positive zero age depth, crustal thickness, and geoid anomalies. Thus, the suggestion of an Azores hot and wet spot (34) is modified into the idea of a wet but not particularly hot spot. One implication is that estimates of mantle temperature beneath mid-ocean ridges based on degree of melting and volume of released melt must take into account the areal heterogeneity of upper-mantle composition (particularly in terms of H_2O and other volatiles) and, consequently, of melting temperature. Other implications are that not all hot spots are necessarily loci of unusually high mantle temperature, and that mantle metasomatism related to recent or ancient degassing events

may play the major role in the enhanced melting and crustal swelling associated with some of them.

REFERENCES AND NOTES

1. J. T. Wilson, *Can. J. Phys.* **41**, 863 (1963); *Philos. Trans. R. Soc. London Ser. A* **25**, 145 (1965).
2. W. J. Morgan, *Nature* **230**, 42 (1971); in *The Sea*, C. Emiliani, Ed. (Wiley-Interscience, New York, 1981), vol. 7, p. 443.
3. R. White and D. McKenzie, *J. Geophys. Res.* **94**, 7685 (1989).
4. N. H. Sleep, *ibid.* **95**, 6715 (1990).
5. D. H. Green and A. E. Ringwood, *Earth Planet. Sci. Lett.* **3**, 151 (1967).
6. P. J. Michael and E. Bonatti, *ibid.* **73**, 91 (1985).
7. E. Bonatti and P. J. Michael, *ibid.* **91**, 297 (1989).
8. ———, M. Seyler, in preparation.
9. H. J. B. Dick, R. L. Fisher, W. B. Bryan, *Earth Planet. Sci. Lett.* **69**, 88 (1984).
10. The mineral chemistry of mantle-equilibrated phases olivine, opx, cpx, and spinel changes as a result of increasing degrees of partial melting of the upwelling mantle. The changes reflect the incompatible behavior during melting of some elements such as Al, Ca, Fe, and Na, which partition with the melt, and the refractory behavior of other elements such as Mg and Cr, which stay with the residue. As a result, the spinel $\text{Cr}/(\text{Cr} + \text{Al})$ ratio and the olivine and pyroxene $\text{Mg}/(\text{Mg} + \text{Fe})$ ratios increase in the residual mantle peridotite with increasing degrees of melting, whereas the Al content of pyroxene decreases. If care is taken to avoid mineral chemistry changes due to subsolidus re-equilibration and to low-temperature alteration, and if reasonable assumptions are made concerning initial mantle peridotite composition, degrees of melting can be estimated by calibration of the mineral chemistry data with experimental results (6, 9, 11, 12). The spinel $100 \text{ Cr}/(\text{Cr} + \text{Al})$ ratio found in peridotites from the AHS area (Figs. 1 and 2) correlates directly with the Fo content of olivine and $100 \text{ Mg}/(\text{Mg} + \text{Fe})$ ratio of opx, and inversely with Al content of opx (6–8). These relationships support the concept of a high degree of melting in the AHS area.
11. A. J. Jaques and D. H. Green, *Contrib. Mineral. Petrol.* **73**, 287 (1980).
12. B. O. Mysen and I. Kushiro, *Am. Mineral.* **82**, 52 (1977).
13. P. R. Vogt, in *The Western North Atlantic Region*, vol. M of *The Geology of North America*, P. R. Vogt and B. E. Tucholke, Eds. (Geological Society of America, Denver, CO, 1986).
14. W. F. Haxby, J. A. Andrews, W. R. Buck, *J. Geophys. Res.*, in press.
15. E. M. Klein and C. H. Langmuir, *ibid.* **92**, 8089 (1987). These authors normalized the Na_2O content of basalt to 8% MgO in order to eliminate effects due to low-pressure fractionation.
16. J. G. Schilling *et al.*, *Am. J. Sci.* **283**, 510 (1983).
17. P. R. A. Wells, *Contrib. Mineral. Petrol.* **62**, 129 (1977).
18. D. H. Lindsley, *Am. Mineral.* **68**, 477 (1983).
19. ——— and D. J. Anderson, *J. Geophys. Res.* **88**, suppl. A887 (1983).
20. F. R. Boyd, *Geochim. Cosmochim. Acta* **37**, 2533 (1973).
21. S. K. Saxena, *Earth Planet. Sci. Lett.* **65**, 382 (1983).
22. G. Sen, *Am. Mineral.* **70**, 678 (1985).
23. Temperature estimates from Wells' equations reproduce experimental data within 70°C (17); those from Lindsley's equations are within about 50°C (18, 19). Exsolution of cpx from opx and vice versa tends to lower the estimated temperatures. Low ($\sim 5\%$ by volume) degrees of exsolution are generally evident in pyroxenes from North Atlantic peridotites. No attempt was made to reconstruct pre-exsolution compositions. This effect results in a more or less systematic lowering of the estimated temperatures, which should not significantly affect the trend of relative temperature variations along the MAR upper mantle. Temperatures calculated by the methods of Wells and Lindsley are related, although the Lindsley geothermometer tends to give higher values (Fig. 2) and a higher scatter in each area.
24. Average calculated temperatures for each area (that is, for each fracture zone or ODP site) fall between 945° and 1120°C . The two areas with the lowest average estimated temperatures are the fracture zone at 43°N and DSDP site 556, both within the AHS region. Temperatures $>1150^\circ\text{C}$ have been obtained only from some samples from the Gibbs, Atlantis, and Vema fracture zones that contain low-Ca cpx [with <43 mole percent wollastonite component (wo)], in contrast with diopsidic ($>45\%$ wo) cpx commonly found in oceanic peridotites. These low-Ca cpx appear to be enriched in Fe and Ti relative to common cpx of oceanic peridotites (25). Similar low Ca, high Fe cpx found in peridotite nodules have been attributed to exchange of the peridotite with hot magma intrusions at mantle depth (26).
25. E. Bonatti and M. Seyler, in preparation.
26. J. J. Gurney and B. Harte, *Philos. Trans. R. Soc. London Ser. A* **297**, 273 (1980).
27. Both Wells' (17) and Lindsley's (18, 19) geothermometers estimate the closure temperature of reactions between coexisting opx and cpx in peridotite. The estimated temperatures may be affected by the cooling rate of the upwelling mantle bodies. Cooling rate is affected by upwelling rate [see for instance A. C. Lasaga, in *Kinetics and Equilibrium in Mineral Reactions*, S. K. Saxena, Ed. (Springer-Verlag, New York, 1983), vol. 3, pp. 81–114]. An extreme case is that of mantle xenoliths transported rapidly from the mantle to the surface by basalts or kimberlites. Cooling rates are fast, and the estimated temperature should reflect closely the temperature of the zone where the xenolith originated in the mantle. Large, slowly upwelling mantle bodies (such as those sampled for this study) would instead allow some re-equilibration to occur during slow cooling. Everything else being equal, faster cooling rates would result in higher temperature estimates, because reactions would not be allowed sufficient time to proceed below a given, relatively high, temperature. Rate of upwelling (and rate of cooling) should be higher for a hotter mantle column (mantle plume or hot spot) than for a mantle column within a normal mid-ocean ridge mantle thermal regime. Thus, even if the estimated temperatures are affected by the cooling rate, they should be higher in hot spot areas than in normal regions.
28. M. Obata, *Am. Mineral.* **61**, 804 (1976).
29. D. J. Henry and L. G. Medaris, *Am. J. Sci.* **208A**, 211 (1980).
30. I. Kushiro *et al.*, *J. Geophys. Res.* **73**, 6023 (1968).
31. I. Kushiro, *Am. J. Sci.* **267A**, 263 (1969).
32. P. J. Wyllie, *J. Geophys. Res.* **76**, 1328 (1971).
33. D. H. Green, *Earth Planet. Sci. Lett.* **19**, 37 (1973).
34. B. O. Mysen and A. L. Boettcher, *J. Petrol.* **16**, 520 (1975).
35. P. J. Wyllie, *J. Geophys. Res.* **93**, 4171 (1988).
36. J. G. Schilling, M. B. Bergeron, R. Evans, *Phil. Trans. R. Soc. London Ser. A* **297**, 147 (1980).
37. W. M. White and J. G. Schilling, *Geochim. Cosmochim. Acta* **42**, 1501 (1978).
38. E. Bonatti *et al.*, *J. Geophys. Res.* **31**, 599 (1986).
39. H. K. Brueckner, A. Zindler, M. Seyler, E. Bonatti, *Tectonophysics* **150**, 163 (1988).
40. D. A. Wood, *Geology* **7**, 499 (1979).
41. J. Verhoogen, *Geol. Soc. Am. Bull.* **84**, 515 (1973).
42. R. Grant Cawthorn, *Earth Planet. Sci. Lett.* **27**, 113 (1975).
43. D. McKenzie and M. J. Bickle, *J. Petrol.* **29**, 625 (1988).
44. M. D. Kurz, W. J. Jenkins, J. G. Schilling, S. R. Hart, *Earth Planet. Sci. Lett.* **58**, 1 (1982).
45. H. Craig and J. Lupton, in *The Sea*, C. Emiliani, Ed. (Wiley-Interscience, New York, 1981), vol. 7, pp. 391–428.
46. H. Craig *et al.*, *Geophys. Res. Lett.* **5**, 897 (1978).
47. R. Vollmer, *Geology* **11**, 452 (1983).
48. D. K. Bailey, *Nature* **296**, 525 (1982); F. E. Lloyd and D. K. Bailey, *Phys. Chem. Earth* **9**, 626 (1975).
49. J. E. Lupton *et al.*, *Nature* **266**, 244 (1977).
50. J. B. Dawson and J. V. Smith, *Contrib. Mineral. Petrol.* **100**, 510 (1988).
51. M. J. Norry *et al.*, *Philos. Trans. R. Astron. Soc. Ser. A* **297**, 123 (1980).
52. E. Bonatti, *J. Geophys. Res.* **76**, 3825 (1978).
53. D. McKenzie and R. K. O'Nions, *Nature* **301**, 229 (1983).
54. S. B. Shirley *et al.*, *ibid.* **325**, 217 (1987).

55. W. G. Melson, S. R. Hart, G. Thompson, *Geol. Soc. Am. Mem.* **132**, 241 (1972).
56. M. K. Roden, S. R. Hart, G. Thompson, *Contrib. Mineral. Petrol.* **85**, 376 (1984).
57. E. Bonatti, *Nature* **345**, 800 (1990).
58. T. Staudacher *et al.*, *Earth Planet. Sci. Lett.* **96**, 119 (1989).
59. M. J. O'Hara, *Nature* **253**, 708 (1975); F. R. Boyd and R. B. McCalister, *Geophys. Res. Lett.* **3**, 509 (1976).
60. H. B. Dick and T. Bullen, *Contrib. Mineral. Petrol.* **86**, 54 (1984).
61. T. Shibata and G. Thompson, *ibid.* **93**, 144 (1986).
62. I am grateful to G. Ottonello, F. Sciuto, and R. Saxena for help in the geothermometry section, and to D. Walker and two anonymous reviewers for constructive comments. I thank D. Breger, P. Catanzaro, and K. Streech for help in putting together the manuscript. Research supported by the National Science Foundation. Lamont-Doherty Geological Observatory of Columbia University Contribution no. 4665.

14 May 1990; accepted 17 July 1990

Hematite Nanospheres of Possible Colloidal Origin from a Precambrian Banded Iron Formation

JUNG HO AHN* AND PETER R. BUSECK

Exceptionally small spheres (nanospheres) of hematite (diameters between 120 and 200 nanometers) occur in the Marra Mamba Iron Formation of the Hamersley Basin, Australia. The nanospheres are clustered into small aggregates and may have formed by structural ordering and dehydration of colloidal iron hydroxide particles. Individual spheres consist of numerous thin, curved hematite platelets surrounding a central void that is approximately half the diameter of the sphere; this texture suggests that they formed by a volume reduction of the original colloidal particles by ~12.5%. The occurrence of hematite nanospheres supports the hypothesis that some of the iron was deposited colloiddally during the development of banded iron formations, approximately 2.5 billion years ago.

THE ORIGIN OF PRECAMBRIAN IRON formations, the world's oldest and largest iron deposits, has been a source of continuing interest and occasional controversy for many decades (1-6). They occur as layered rocks on all continents and provide the bulk of mined iron. Potentially, they indicate the character and history of the early Earth's oceans, atmosphere, and biosphere (5-9); they have been used to infer the evolution of Earth's atmosphere in Precambrian time. The methods of concentrating, transporting, and then depositing the vast quantities of iron in these extensive sedimentary units provide serious geological and geochemical problems.

Colloidal transport and deposition has been proposed as one means of moving the extraordinary amounts of iron to the basins where the iron ultimately was deposited (10, 11), but direct observational evidence has been both sparse and equivocal. Spherical structures 5 to 40 μm in diameter are common in iron formations, but there is dispute over whether they indicate purely chemical colloidal processes (12-15), organic activity (16), or recrystallization (17). In this paper we describe tiny hematite spheres that have

diameters only 1/40 to 1/200 of known spherical features in iron formations. We propose these spheres as strong indicators of colloidal processes during deposition of the iron formations.

We studied two samples that were selected to be representative of regions of drill core separated vertically by ~2 m. The core (D.D.H. No. 270, located 38 km west of Wittenoom, Australia) is from the Marra Mamba Iron Formation, which is of the Lake Superior type (17a). This formation was deposited about 2.5 billion years ago, at the approximate boundary between the Archean and Proterozoic ages and is the lowermost member of the Hamersley Group of Western Australia (18). In addition to the hematite, the samples contain quartz, magnetite, stilpnomelane, ankerite, minnesotaite or talc, and fibrous riebeckite (crocidolite). Specimens were examined at 400 and 120 kV with JEOL JEM-4000EX and Philips 400T transmission electron microscopes (19).

In all the grains that we observed, the hematite occurs in tiny clusters between quartz grains. Most hematite aggregates are smaller than 2 μm in diameter, and they have relatively sharp boundaries with the quartz (Fig. 1). Electron-diffraction patterns show rings as a result of the polycrystalline character of the aggregates (Fig. 2 and Table 1). These aggregates consist of spheres that have diameters between 120 and 200 nm (Fig. 3); we call them "nanospheres." The

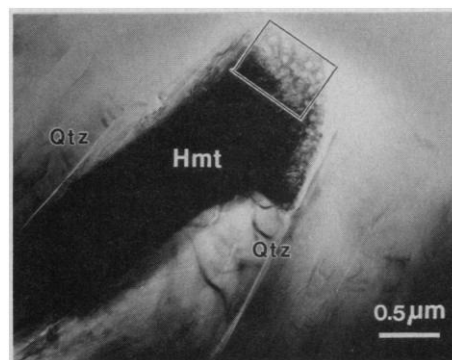


Fig. 1. Low-magnification TEM image showing a hematite cluster (Hmt) in quartz (Qtz).

hematite nanosphere clusters are widespread in the specimens we studied. Only circular shapes were observed in our transmission electron microscopy (TEM) images, indicating that the hematite has a spherical rather than cylindrical form.

The TEM images of the nanospheres show marked contrast between the outer shells and central areas (Fig. 3). These cores show light contrast and produce neither electron-diffraction patterns nor lattice fringes in TEM observations; only the outer shells consist of hematite. These shells consist of thin, subparallel, platy crystals, each approximately 3 to 5 nm thick (Fig. 4). Completely circular single crystals were not observed; instead, many curved crystals are joined to form spherical structures.

The appearance of the hematite nanospheres is similar to that of Fe-Si-Al-oxyhydroxides that crystallized from gel spheres (20). The presence of central voids suggests that the nanospheres also formed by void nucleation (21) from colloidal gels rather than by nucleation crystallization or spinodal decomposition. The central voids apparently formed during shrinkage caused by both ordering and dehydration.

Fine-grained hematite in weakly meta-

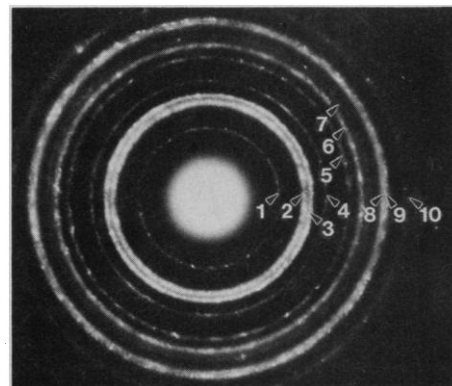


Fig. 2. Electron-diffraction pattern of hematite showing ring features. The ten innermost reflection rings are numbered; their interplanar spacings and indices are given in Table 1.

J. H. Ahn, Department of Geology, Arizona State University, Tempe, Arizona, 85287-1404.
P. R. Buseck, Departments of Geology and Chemistry, Arizona State University, Tempe, Arizona 85287-1404.

*Present address: Korea Ocean Research and Development Institute, Ansan P.O. Box 29, Seoul, Korea.